



COMMUNICATIONS PHYSICS

ARTICLE

<https://doi.org/10.1038/s42005-019-0184-y>

OPEN

Inelastic collapse of perfectly inelastic particles

Nikola Topic¹ & Thorsten Pöschel ²

One of the most intensively discussed subjects in the dynamics of dissipative hard sphere systems is the effect of inelastic collapse, where the entire kinetic energy of the relative motion of a set of particles is dissipated in finite time due to an infinite sequence of collisions. The known collapse scenarios imply two preconditions: inertia of the particles and at least some degree of elasticity. For completely inelastic particles, collapse scenarios degenerate to a single sticky contact. By considering the overdamped motion of a frictional particle along the steepest descent in a rigid landscape, here we show that there exist collapse scenarios of novel type even if neither of these preconditions hold true. By means of numerical simulations we show that such collapses are no rare events due to particular particle shape and/or initial conditions and, thus, may be considered as an alternative scenario of granular cluster formation.

¹Institute for Fluid Mechanics, Friedrich-Alexander-Universität Erlangen-Nürnberg, Cauerstraße 4, 91058 Erlangen, Germany. ²Institute for Multiscale Simulation, Friedrich-Alexander-Universität Erlangen-Nürnberg, Cauerstraße 3, 91058 Erlangen, Germany. Correspondence and requests for materials should be addressed to T.P. (email: thorsten.poeschel@fau.de)

The problem of inelastic collapse of identical, ideally hard, purely repulsive, and dissipatively colliding spheres reads as follows: given N particles in force-free space, are there initial conditions for the positions and velocities such that the entire energy of their relative motion will be dissipated? If dissipation is quantified by the coefficient of restitution, ε , relating the pre-collisional and post-collisional normal velocity, the question implies that there occurs an infinite sequence of collisions resulting in a cluster where each particle is in permanent contact with at least one neighbor. The answer to the question is “yes”, provided the coefficient of restitution does not exceed a certain limit, $\varepsilon = 7 - 4\sqrt{3}^{1-3}$. This result, obtained first for the case of three aligned particles attracted much attention and subsequently many related phenomena were studied, for instance the one-dimensional collapse of N particles^{4,5}, frictional particles⁶, non-perfectly aligned particles⁷, collapses in two and three-dimensional systems⁸, in the presence of solid walls^{9–11}, under the influence of noise^{5,12–15}, and others. While collapse phenomena seem to be omnipresent for simple particles, the effect may be suppressed for more complex particles, for instance when the coefficient of restitution depends on the impact rate¹⁶ or for particles having internal degrees of freedom¹⁷.

While the mathematical existence of inelastic collapse scenarios is free of doubt, the implications of a collapse for the physics of dissipative gases of hard spheres, frequently called granular gases, is still under debate, for example, see refs. 18–20. An extended discussion on the collapse and its relation to granular clustering^{2,21}, can be found in ref. 22.

The infinite sequence of collisions leading to a collapse occurs in finite time^{1,3} which lead to severe problems for event-driven molecular dynamics where time progresses in steps of collisions. There are several numerical tricks, which, however, fail in certain situations^{23,24} or change the dynamics in an undesired way^{25,26}. An event driven algorithm following the dynamics consistently must come to rest (that is, cannot propagate in time) due to the inelastic collapse²⁷.

A close relative to the inelastic collapse revealing all its interesting features²⁰ is the problem of an ideally hard particle dropped from height h_0 to a plane where dissipation is again described by the coefficient of restitution, ε . The particle performs an infinite number of jumps of height $h_{n+1} = \varepsilon^2 h_n$ ($n = 0 \dots \infty$) in finite time $\sqrt{2h_0/g}(1 + \varepsilon)/(1 - \varepsilon)$, where g is gravity.

Common to all collapse scenarios are two preconditions: (a) a certain degree of elasticity is needed and (b) the dynamics must be inertial. If violated, the sequence of collisions terminates after the first contact and the collapse scenario renders trivial.

In the present work, we show that for complex shaped, frictional particles moving in a rigid landscape with overdamped dynamics, there exist collapse scenarios, although both preconditions, (a) and (b), are not fulfilled. In the course of such a collapse, the particle experiences an infinite number of collisions occurring in finite time, in that, these scenarios resemble the collapse scenarios discussed above.

Results

Collapse in numerical simulations. To demonstrate the effect, particles as shown in Fig. 1 each consisting of four spheres are dropped from a point source to pile up to a heap due to the Visscher-Bolsterli algorithm^{28,29}. Each dropped particle moves in the landscape formed by previously sedimented particles (see Fig. 1) until it finds its stable position in a local minimum. The dynamics is assumed overdamped, e.g., under the influence of an ambient viscous fluid³⁰, corresponding to vanishing coefficient of restitution, $\varepsilon = 0$, irrespective of the particle material properties since the particles move always at terminal velocity, in the limit of

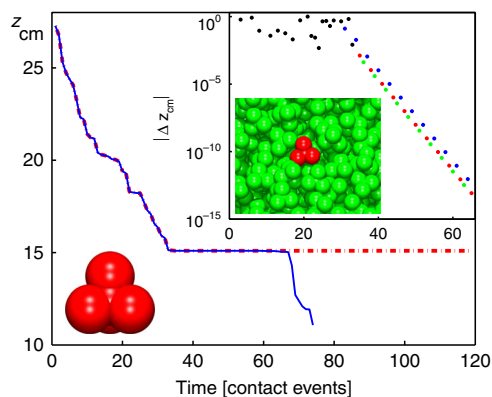


Fig. 1 Particle descending in a complex landscape. A particle (lower inset) topples down a heap formed by identical, previously sedimented particles. The upper inset shows part of the heap’s surface with the currently moving particle drawn in red. Blue and red lines: Vertical component of the particle’s center of mass, z_{cm} , over time in units of contact events. The dashed line shows the collapse scenario, the full line shows z_{cm} with the regularization described in the text. Circles: decrement $|\Delta z_{cm}|$ of z_{cm} in logscale. The color of the data points indicate the active contact. We see that for $t \geq 33$ the motion is regular and cyclic

large damping. Note that for the limit of large damping, long-range forces and lubrication forces vanish. No slip is assumed for the contact between the particle and the landscape. Consequently, due to overdamped dynamics where inertial forces are unimportant, the motion of the particle is solely determined by the instantaneous force, that is, by the gradient of the potential. Once a contact is established, the particle rolls such that its center of mass follows the steepest descent.

Figure 1 shows the evolution of the vertical position of the particle’s center of mass following the steepest descent. Time progresses in units of contact events, that is, a data point is drawn whenever a previously open contact between particles closes. At a certain time, $t = 33$, the particle enters a cycling motion, at three contact points in periodic sequence, and eventually experiences a collapse (dashed line) such that the simulation comes to rest. When entering the collapse scenario, the decrements, $|\Delta z_{cm}|$, change qualitatively (Fig. 1): For $t \geq 33$, the decrement becomes regular; here the periodically active contact points are indicated by red, green and blue color. For $t < 33$ other contacts are active (black dots) and the decrement is on the scale of the particle size $|\Delta z_{cm}| \sim 1$.

The situation resembles the collapse scenario for granular gases where an infinite number of collisions (also occurring in cyclic sequence) takes place in finite time^{1–3}, such that event-driven simulations cannot progress beyond this time. For event-driven Molecular Dynamics, the inelastic collapse is a severe problem, therefore, methods were developed^{23–26} to abandon the infinite cyclic sequence by a small perturbation of the system which helps to overcome the collapse without noticeably changing the macroscopic system dynamics.

Similarly, our system cannot progress beyond a collapse as one can see in Fig. 1 (dashed line). Therefore, in simulations we need a way to identify and overcome the collapse. A natural way to identify the contact of two objects is by the vanishing of the distance between their surfaces. In a collapse scenario, however, this condition is approached through an infinite sequence. Therefore, we need another condition to decide when particles touch one another. For the simulation in Fig. 1 (full line), we defined the contacts closed when the distance the center of mass traveled in one cycle drops below 10^{-10} particle diameters. This condition is fulfilled at $t = 66$, where we assume all contacts of the

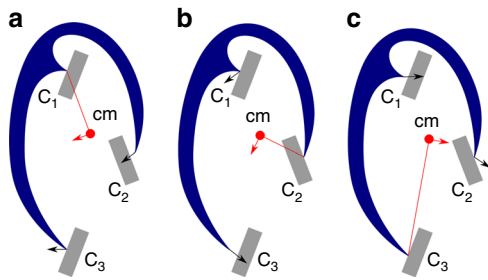


Fig. 2 Contact patches of a complex particle and cyclic motion. A particle (blue) in overdamped motion in a rigid landscape specified by three patches (gray). Panel **a** shows the initial state, with contacts C_1 and C_3 closed and C_2 open. The position is unstable, thus, the particle rolls in C_1 by opening C_3 until C_2 closes, as sketched in panel **b**. Panel **b**: Now the particle rolls in C_2 by opening C_1 until C_3 closes, as sketched in panel **c**. Panel **c**: To close the cycle, the particle rolls in C_3 by opening C_2 until C_1 closes. Now the particle is again in the situation sketched in panel **a**. Red symbols indicate the particle's center of mass, its direction of motion and the current point of rotation. Black arrows show the direction of motion of the particle's edges contacting the landscape in cyclic sequence (a) \rightarrow (b) \rightarrow (c) \rightarrow (a) \rightarrow ...

particle closed and assess whether the particle found a stable position. This is not the case for the situation shown in Fig. 1, $t = 66$, such that the particle continues its motion along the steepest descent, that is, we overcame the collapse. Remarkably, a collapsed position does not necessarily correspond to the minimum of potential energy. Once all three contacts are closed, due to collapse, the particle can continue rolling on two contacts, following the steepest descent.

The described collapse scenario could be observed for many particle shapes, except for particles whose surface is convex everywhere.

We wish to point out that the described model was successfully applied to a wide class of sedimentation phenomena with applications, ranging from geophysical systems^{31,32} to nano-structured materials^{29,33}. The numerical method was first described for spheres²⁸ and later generalized to more complex particles^{29,34}.

Analytical characterization. We assume a particle shape as sketched in Fig. 2 which may look rather artificial but allows us to introduce the notation in a simple way. We will show that its motion along the steepest descent has the same properties as the motion of the particle in the sedimentation process presented above.

Consider the steepest descent of the particle in a landscape indicated by three patches, shown in Fig. 2.

Figure 2a shows the initial state, with contacts C_1 and C_3 closed and C_2 open. The position is unstable, thus, the particle rolls in C_1 by opening C_3 until C_2 closes, Fig. 2b. Now the particle rolls in C_2 by opening C_1 until C_3 closes, Fig. 2c. To close the cycle, the particle rolls in C_3 by opening C_2 until C_1 closes. Now the particle is again in the situation sketched in Fig. 2a and the sequence repeats cyclically. Note that each step of this motion is related to lowering the center of mass, thus, each of the situations, Fig. 2a–c is unstable. The cycling motion terminates when simultaneously all three contacts are closed.

For quantitative analysis of the cyclic motion, we consider the evolution of the gap sizes g_i for one cycle. Here, g_i denotes the distance of the tip of the particle at contact i in the state when the contact is fully open, see Fig. 3. Consider one cycle, starting at the position shown in Fig. 2a. The ratio of initial gap size, g_2 , and

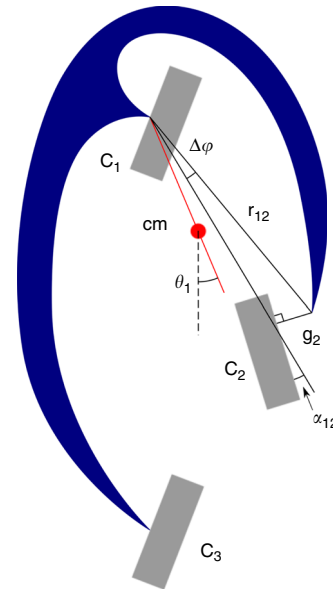


Fig. 3 Relation between g_2 and $\Delta\varphi$. Relation between g_2 (distance of the tip of the particle and contact point C_2 in the state when the contact is fully open) and $\Delta\varphi$ (related rotation angle of the particle). α_{12} is the angle between the surface C_2 and the line connecting the rotation point, C_1 , with the point where particle will contact the surface at C_2 . θ_1 is the angle between the vertical (dashed line) and the line connecting the center of mass with C_1

the corresponding gap size in the successive cycle, g'_2 reads

$$\frac{g'_2}{g_2} = \frac{g'_2 g_1 g_3}{g_1 g_3 g_2} \quad (1)$$

In order to obtain g_3/g_2 we look to the motion starting from the initial position, Fig. 2a, and the related rotation of the particle by the angle $\Delta\varphi$, see Fig. 3.

Assuming the gap size much smaller than the particle size, $g_2 \ll r_{12}$, we obtain in a linear approximation

$$\Delta\varphi = \frac{g_2}{r_{12} |\cos \alpha_{12}|} \quad (2)$$

where r_{ij} is the distance between the current point of rotation, C_i , and the tip of the particle at the open contact, C_j . α_{ij} is the angle between the surface C_j and the line connecting the rotation point, C_i , with the point where the particle will contact the surface at C_j . Figure 3 sketches the introduced variables.

At the same time the tip of the particle at position C_3 is also rotated by $\Delta\varphi$ around C_1 , therefore,

$$\frac{g_3}{r_{13} |\cos \alpha_{13}|} = \Delta\varphi = \frac{g_2}{r_{12} |\cos \alpha_{12}|} \quad (3)$$

$$\frac{g_3}{g_2} = \frac{r_{13} |\cos \alpha_{13}|}{r_{12} |\cos \alpha_{12}|} \quad (4)$$

The other quantities needed for Eq. (1), g_1/g_3 and g'_2/g_1 , can be obtained in the same way by cyclic change of indexes. With $r_{ij} = r_{ji}$ we obtain from Eq. (1):

$$\delta \equiv \frac{g'_2}{g_2} = \frac{r_{32} |\cos \alpha_{32}| r_{21} |\cos \alpha_{21}| r_{13} |\cos \alpha_{13}|}{r_{31} |\cos \alpha_{31}| r_{23} |\cos \alpha_{23}| r_{12} |\cos \alpha_{12}|} = \frac{|\cos \alpha_{32}| |\cos \alpha_{21}| |\cos \alpha_{13}|}{|\cos \alpha_{31}| |\cos \alpha_{23}| |\cos \alpha_{12}|} \quad (5)$$

This recursion relation obtained for g'_2/g_2 holds also true for the other gap sizes as can be seen by cyclically permuting the indexes $\{1, 2, 3\} \rightarrow \{2, 3, 1\} \rightarrow \{3, 1, 2\}$. Therefore, for $\delta < 1$, in each cycle

the gaps will reduce in geometric progression, thus, the series $g \rightarrow (g' = \delta g) \rightarrow (g'' = \delta^2 g) \rightarrow \dots$, converges to zero and the motion of the particle comes to rest after an infinite number of cycles when all contacts are closed, $(g_1, g_2, g_3) \rightarrow 0$. It may be shown that δ given by Eq. (5) is always smaller than unity, consequently, if the particle performs one full cycle, it will necessarily enter a collapse scenario.

To compute the total distance traveled by the center of mass during the collapse scenario, again we consider the situation sketched in Fig. 2a. Since $g_2 \ll r_{12}$ (and likewise for the other gaps), \mathbf{r}_{cm} moves along straight lines. The distance traveled during the first cycle, is

$$\Delta r_{cm}^{(1)} \equiv |\Delta \mathbf{r}_{cm}^{(1)}| = \Delta_1 r_{cm}^{(1)} + \Delta_2 r_{cm}^{(1)} + \Delta_3 r_{cm}^{(1)}, \quad (6)$$

where subscripts denote the contact in which the particle rolls. From geometry we obtain

$$\Delta_1 r_{cm}^{(1)} = |\Delta \varphi_1| r_{1cm} = \frac{r_{1cm}}{|r_{12} \cos \alpha_{12}|} g_2 \quad (7)$$

and likewise $\Delta_2 r_{cm}^{(1)}$ and $\Delta_3 r_{cm}^{(1)}$ with cyclic permutation of the indexes where r_{icm} is the distance between contact C_i and the center of mass.

With Eq. (5), we obtain a recursion relation for the motion of the center of mass during the k th cycle, $\Delta r_{cm}^{(k)} = \delta \Delta r_{cm}^{(k-1)} = \delta^{(k-1)} \Delta r_{cm}^{(1)}$. Summing up, we obtain the total path traveled by the center of mass:

$$\Delta r_{cm}^{tot} = \sum_{k=1}^{\infty} \Delta r_{cm}^{(k)} = \frac{\Delta r_{cm}^{(1)}}{1 - \delta}. \quad (8)$$

The distance traveled in vertical direction during the first cycle is

$$\Delta z_{cm}^{(1)} = \Delta_1 r_{cm}^{(1)} |\sin \theta_1| + \Delta_2 r_{cm}^{(1)} |\sin \theta_2| + \Delta_3 r_{cm}^{(1)} |\sin \theta_3|, \quad (9)$$

where angles θ_i are defined in Fig. 3. The total descent is, therefore,

$$\Delta z_{cm}^{tot} = \Delta z_{cm}^{(1)} (1 - \delta)^{-1} \quad (10)$$

The analysis presented here applies to a wider class of systems: Indeed, the characteristic that the systems from Figs. 1 and 2 share that leads them to collapse is the identical relation for opening/closing contacts (up to permutation of (C_1, C_2, C_3)): rolling on C_1 implies $(\dot{g}_1 = 0; \dot{g}_2 < 0; \dot{g}_3 > 0)$, rolling on C_2 implies $(\dot{g}_1 > 0; \dot{g}_2 = 0; \dot{g}_3 < 0)$, rolling on C_3 implies $(\dot{g}_1 < 0; \dot{g}_2 > 0; \dot{g}_3 = 0)$, representing, thus, together with $\delta < 1$ sufficient conditions for the collapse. For collapse scenarios involving three contacts, these conditions are also necessary –if any of them is violated, the sequence ceases. There may, however, exist more complex scenarios involving more than three contacts obeying different rules.

We wish to mention that there is a difference between the behavior of two and three-dimensional systems. Indeed, in three dimensions, a particle can undergo a collapse scenario and end up in a situation where all contacts are closed but the particle's position is not stable. This is, what we see in Fig. 1 at time $t \approx 66$. In this case, after a collapse, the particle continues its descent in the landscape created by previously sedimented particles until it either finds its stable position or again undergoes a collapse after which it may be in a stable or unstable position. In contrast, in a two-dimensional system, a collapse scenario leads always to a stable position. Nevertheless, while the post-collapse behavior may be different in two-dimensional and three-dimensional systems, the mechanism of the collapse scenario described in this section is the same.

Numerical test. We assume the system sketched in Fig. 2a with the initial positions of the contact points and the center of mass

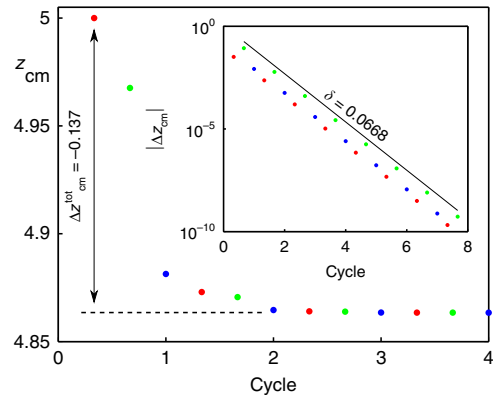


Fig. 4 Evolution of the vertical position of the center of mass. Evolution of the vertical position of the center of mass, z_{cm} . There are three data points per cycle, due to the periodic motion characterized by closing and opening contacts C_1, C_2 , and C_3 , indicated by color. Inset: decrements $|\Delta z_{cm}|$ with the fit $\Delta z_{cm}^{(i)} \sim \delta^{i-1}$, where i is the index of the cycle

$C_1 = (0;10), C_2 = (5;5), C_3 = (0;0)$, and $\mathbf{r}_{cm} = (5/3;5)$. The surface patches are inclined by 60° with respect to the horizontal. The initial position of the tip of the particle close to C_2 is $(5.1;5.1)$. Starting from this initial configuration, in agreement with (8), the vertical component of the center of mass decays and saturates at a finite value while the decrements $-\Delta z_{cm}$ in each cycle decay exponentially, Fig. 4. Thus, after an infinite number of cycles, the particle assumes a position with all three contacts closed.

For the specified situation, from Eq. (5) we obtain an analytic expression for the recursion parameter, $\delta \approx 0.066796$, in good agreement with the fit shown in Fig. 4.

The described collapse scenario is not an exotic phenomenon occurring for a small set of particular initial conditions. To estimate the frequency of occurrence, we generated 10^9 sets of system configurations specified by the positions of C_1, C_2, C_3 , and \mathbf{r}_{cm} all chosen randomly from the interval $[0, 1]$, and slopes of the surface patches from $[-\pi/2, \pi/2]$. Out of this set, approximately 3.6×10^6 systems led to a collapse. Given that a granular system may consist of many millions of complex shaped particles²⁹, therefore, collapse scenarios are no rare events but will occur almost certainly in medium and large scale systems. Similar as for the known inelastic collapse in granular gases, a numerical simulation fails if the system enters a collapse scenario, since due to the infinite sequence of cycles, the algorithm would not progress in (real) time.

Discussion

Inelastic collapse scenarios of dissipative and purely repulsive hard-sphere systems, as extensively discussed in the literature so far, may be described as cyclic sequences of pairwise particle contacts. When a collapse occurs, an infinite sequence of collisions takes place in finite time such that eventually all energy of the relative velocity ceases. Perfectly inelastic particles interacting with coefficient of restitution, $\varepsilon = 0$, cannot undergo such an infinite sequence since the relative velocity of the particles would vanish already after the first contact. For the same reason, non-inertial (overdamped) systems cannot cyclically collapse.

In the present work, we describe a novel collapse scenario occurring for a particle moving along the path of steepest descent of potential energy in a rigid landscape. The particle is assumed perfectly inelastic, $\varepsilon = 0$, and the dynamics is assumed overdamped, such that both preconditions of collapsing mentioned above do not hold true. For a model particle we could rigorously show that the collapse occurs via an infinite cyclic sequence of contacts where the decrement of the vertical component of the

center of mass decreases geometrically such that the infinite sum of the decrements converges to a finite value.

Our model assumes a rigid particle moving in a rigid landscape. For finite stiffness, in the first stage of the scenario, the gap size decays exponentially, since the mechanism driving the cycling motion is not affected by finite stiffness. Later, however, the sequence ceases, when the gap size approaches the typical deformation of particles in contact. Therefore, for finite stiffness, up to this criterion fulfilled, the arguments of our analysis remain invariant.

By extensive numerical simulations we showed that the collapse is not an exotic phenomenon but occurs for a non-negligible fraction (ca. 0.4%) of randomly generated initial conditions for our model particle. It was also shown that the phenomenon occurs for rather common systems, that is, for a particle consisting of five spheres toppling down the surface of a heap built from identical particles.

By now, the theoretically predicted phenomenon was not reported in the experimental literature. We believe that good candidates for experimental confirmation would be the analysis of the sound emission of a particle during sedimentation or the analysis of time series from electrical impedance measurements.

Data availability

All relevant data are available from the authors.

Received: 17 December 2018 Accepted: 13 June 2019

Published online: 23 July 2019

References

- Shida, K. & Kawai, T. Cluster formation by inelastically colliding particles in one-dimensional space. *Phys. A* **162**, 145–160 (1989).
- McNamara, S. & Young, W. R. Inelastic collapse and clumping in a one-dimensional granular medium. *Phys. Fluids* **4**, 496–504 (1992).
- Constantin, P., Grossman, E. & Mungan, M. Inelastic collisions of three particles on a line as a two-dimensional billiard. *Phys. D* **83**, 409–420 (1995).
- Cipra, B., Dini, P., Kennedy, S. & Kolan, A. Stability of one-dimensional inelastic collision sequences of four balls. *Phys. D* **125**, 183–200 (1999).
- Benedetto, D. & Caglioti, E. The collapse phenomenon in one-dimensional inelastic point particle systems. *Phys. D* **132**, 457–475 (1999).
- Schörghofer, N. & Zhou, T. Inelastic collapse of rotating spheres. *Phys. Rev. E* **54**, 5511–5515 (1996).
- Zhou, T. & Kadanoff, L. P. Inelastic collapse of three particles. *Phys. Rev. E* **54**, 623–628 (1996).
- McNamara, S. & Young, W. R. Inelastic collapse in two dimensions. *Phys. Rev. E* **50**, R28–R31 (1994).
- Bernu, B. & Mazighi, R. One-dimensional bounce of inelastically colliding marbles on a wall. *J. Phys. A* **23**, 5745–5754 (1990).
- McNamara, S. The onset of inelastic collapse in a one-dimensional granular gas. *Gran. Matter* **14**, 121–126 (2012).
- Gao, M., Wylie, J. J. & Zhang, Q. Inelastic collapse in a corner. *Commun. Pure Appl. Anal.* **8**, 275–293 (2009).
- Burkhardt, T. W. & Kotsev, S. N. Equilibrium of a confined, randomly accelerated, inelastic particle: Is there inelastic collapse? *Phys. Rev. E* **70**, 026105 (2004).
- Cornell, S. J., Swift, M. R. & Bray, A. J. Inelastic collapse of a randomly forced particle. *Phys. Rev. Lett.* **81**, 1142–1145 (1998).
- Florencio, J., Sá Barreto, F. C. & de Alcantara Bonfim, O. F. Comment on ‘Inelastic collapse of a randomly forced particle’. *Phys. Rev. Lett.* **84**, 196–196 (2000).
- Anton, L. Noncollapsing solution below r_c for a randomly forced particle. *Phys. Rev. E* **65**, 047102 (2002).
- Goldman, D. et al. Absence of inelastic collapse in a realistic three ball model. *Phys. Rev. E* **57**, 4831–4833 (1998).
- Paparella, F. & Passoni, G. Absence of inelastic collapse for a 1D gas of grains with an internal degree of freedom. *Comput. Math. Appl.* **55**, 218–229 (2008).
- Kadanoff, L. Built upon sand: Theoretical ideas inspired by the flow of granular materials. *Rev. Mod. Phys.* **71**, 435–444 (1999).
- Alam, M. & Hrenya, C. M. Inelastic collapse in simple shear flow of a granular medium. *Phys. Rev. E* **63**, 061308 (2001).
- Goldhirsch, I. Introduction to granular temperature. *Powder Technol.* **182**, 130–136 (2008).
- Goldhirsch, I. & Zanetti, G. Clustering instability in dissipative gases. *Phys. Rev. Lett.* **70**, 1619–1622 (1993).
- Goldhirsch, I. Rapid granular flows. *Annu. Rev. Fluid Mech.* **35**, 267–293 (2003).
- Pöschel, T. & Schwager, T. *Computational Granular Dynamics: Models and Algorithms* (Springer, Berlin, 2005).
- Reichardt, R. & Wiechert, W. Event driven algorithms applied to a high energy ball mill simulation. *Gran. Mat.* **9**, 251–266 (2007).
- Deltour, P. & Barrat, J. L. Quantitative study of a freely cooling granular medium. *J. Phys. I* **7**, 137–151 (1997).
- Luding, S. & McNamara, S. How to handle the inelastic collapse of a dissipative hard-sphere gas with the tc model. *Granul. Matter* **1**, 113–128 (1998).
- Bannerman, M. N., Strobl, S., Formella, A. & Pöschel, T. Stable algorithm for event detection in event-driven particle dynamics. *Comput. Part. Mech.* **1**, 191–198 (2014).
- Visscher, W. M. & Bolsterli, M. Random packing of equal and unequal spheres in two and three dimensions. *Nature* **239**, 504–507 (1972).
- Schwager, T., Wolf, D. E. & Pöschel, T. Fractal substructure of a nanopowder. *Phys. Rev. Lett.* **100**, 218002 (2008).
- Kurita, R. & Weeks, E. R. Experimental study of random-close-packed colloidal particles. *Phys. Rev. E* **82**, 011403 (2010).
- van Rompaey, A. J. J., Verstraeten, G., van Oost, K., Govers, G. & Poesen, J. Modelling mean annual sediment yield using a distributed approach. *Earth Surf. Process. Landf.* **26**, 1221–1236 (2001).
- Lancaster, S. T., Hayes, S. K. & Grant, G. E. Modeling sediment and wood storage and dynamics in small mountainous watersheds. In *Geomorphic Processes and Riverine Habitat*, Vol. 4 of *Water Science and Application* (eds Dorava, J. M., Montgomery, D. R., Palcsak, B. B. & Fitzpatrick, F. A.) 85–102 (American Geophysical Union, Washington, 2013).
- Benabbou, A., Borouchaki, H., Laug, P. & Lu, J. Geometrical modeling of granular structures in two and three dimensions. Application to nanostructures. *Int. J. Numer. Meth. Engng.* **80**, 425–454 (2009).
- Coelho, D., Thovert, J.-F. & Adler, P. M. Geometrical and transport properties of random packings of spheres and aspherical particles. *Phys. Rev. E* **55**, 1959–1978 (1997).

Acknowledgements

We thank the Deutsche Forschungsgemeinschaft (DFG, German Science Foundation) for funding through grant 377472739/GRK2423/1-2019. Support from ZISC and IZ-FPS at FAU Erlangen-Nürnberg is gratefully acknowledged.

Author contributions

N.T. and T.P. designed the research, performed the research, analyzed the data, and wrote the paper.

Additional information

Competing interests: The authors declare no competing interests.

Reprints and permission information is available online at <http://npg.nature.com/reprintsandpermissions/>

Publisher's note: Springer Nature remains neutral with regard to jurisdictional claims in published maps and institutional affiliations.



Open Access This article is licensed under a Creative Commons Attribution 4.0 International License, which permits use, sharing, adaptation, distribution and reproduction in any medium or format, as long as you give appropriate credit to the original author(s) and the source, provide a link to the Creative Commons license, and indicate if changes were made. The images or other third party material in this article are included in the article's Creative Commons license, unless indicated otherwise in a credit line to the material. If material is not included in the article's Creative Commons license and your intended use is not permitted by statutory regulation or exceeds the permitted use, you will need to obtain permission directly from the copyright holder. To view a copy of this license, visit <http://creativecommons.org/licenses/by/4.0/>.

© The Author(s) 2019